PHYSICS AND CHEMISTRY OF SOLID STATE
V. 22, No. 1 (2021) pp. 117-122
Section: Physics

DOI: 10.15330/pcss.22.1.117-122

Vasyl Stefanyk Precarpathian National University

ФІЗИКА І ХІМІЯ ТВЕРДОГО ТІЛА
Т. 22, № 1 (2021) С. 117-122
Фізико-математичні науки

PACS: 31.15.E−, 78.20.Ci ISSN 1729-4428

H. Ilchuk, M. Solovyov, I. Lopatynskyi, F. Honchar, F. Tsyupko

First Principles DFT Calculations of the Optical Properties of A_4BX_6 Group Crystals

Lviv Polytechnic National University, Lviv, Ukraine, mvsolovyov@ukr.net

The results of investigating of the electron band energy structure and optical properties of A_4BX_6 (Tl_4HgI_6 and Tl_4CdI_6) group crystals are presented. The energy band structures of Tl_4HgI_6 and Tl_4CdI_6 crystals are calculated from the first principles within generalized gradient approximation (GGA). The band structure and reflection index were calculated using a pseudopotential method in the framework of density functional theory. Optical absorption edge in Tl_4HgI_6 and Tl_4CdI_6 is formed by direct optical transitions. The spectral dependence of the reflection index was calculated on the basis of the energy band results with using the Kramers–Kronig method. The spectra show pronounced anisotropy in $E\|\boldsymbol{a}(\boldsymbol{b})$ and $E\|\boldsymbol{c}$ polarizations. It was found the anomalous by large values of the birefringence ($\Delta n > 0.18$ for Tl_4HgI_6 and $\Delta n > 0.03$ for Tl_4CdI_6) in the visible and near infrared region.

Keywords: optical constants, birefringence, electron band-energy structure.

Received 28 December 2020; Accepted 25 February 2021.

Introduction

Searching for new functional materials and ways to control their properties belongs to the primary tasks of physics of semiconductors and insulators. Wide-gap semiconductor crystals have been used extensively in X- and γ-ray detectors, the chemical industry, and biomedicine [1-4]. Designing room temperature radiation detectors is an urgent problem of materials science. The A_4BX_6 crystals has a wide band gap (E_g = 2.08 eV [5] for Tl_4HgI_6 and E_g = 2.83 eV [6] for Tl_4CdI_6). The presence of thallium enhances the X- and γ-ray absorption coefficient of the material due to the high density (ρ = 7.19 g/cm^3 [7] for Tl_4HgI_6 and ρ = 6.87 g/cm^3 [7] for Tl_4CdI_6) and large atomic number Z (Z_{Tl} = 81, Z_{Hg} = 80, Z_{Cd} = 48, and Z_I = 53).

By now, the optical, mechanical, spectral, and energetic characteristics of the A_4BX_6 crystals have been well-investigated [2]-[14]. The energy band spectrum [6, 11, 13, 14] is calculated using the local density approximation (LDA) and exchange correlation functional based on the generalized gradient approximation (GGA) in the Perdew, Burke, and Ernzerhof (PBE) parametrization.

For today we have not found in literature any work either theoretical or experimental on birefringence (BRF) of A_4BX_6 group crystals (except Tl_4HgI_6 [13]). In this paper, we presented the results of calculations of the optical constants of BRF of A_4BX_6 crystals.

I. Theoretical Calculation Technique

The theoretical calculations were made using the electron density functional theory (DFT). For ionic potentials, the ultrasoft Vanderbilt pseudopotentials were used [15]. To describe the exchange correlation energy of the electron subsystem, the GGA functional with the PBE parameterization [16] was used. To determine the difference between the experimental [7] and equilibrium theoretical lattice parameters (see Fig. 1 and Table 1), we used the structure-optimization procedure, which consists of finding the minimum full energy as a function of the crystal unit-cell volume [17].

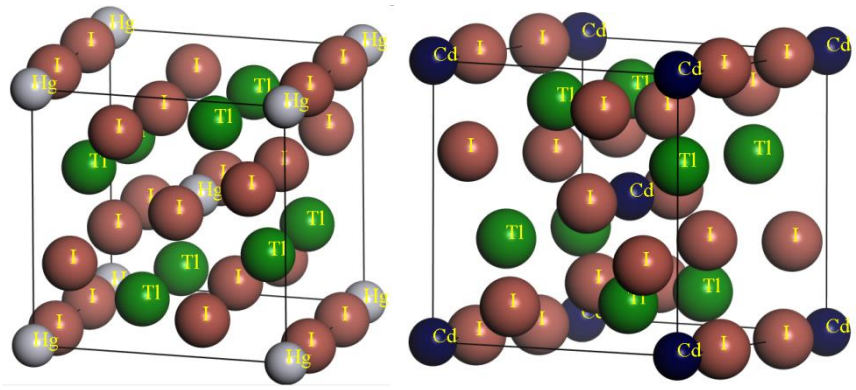

1 2

Fig. 1. Views of the initially optimized structure of the Tl_4HgI_6 (1) and Tl_4CdI_6 (2) crystals.

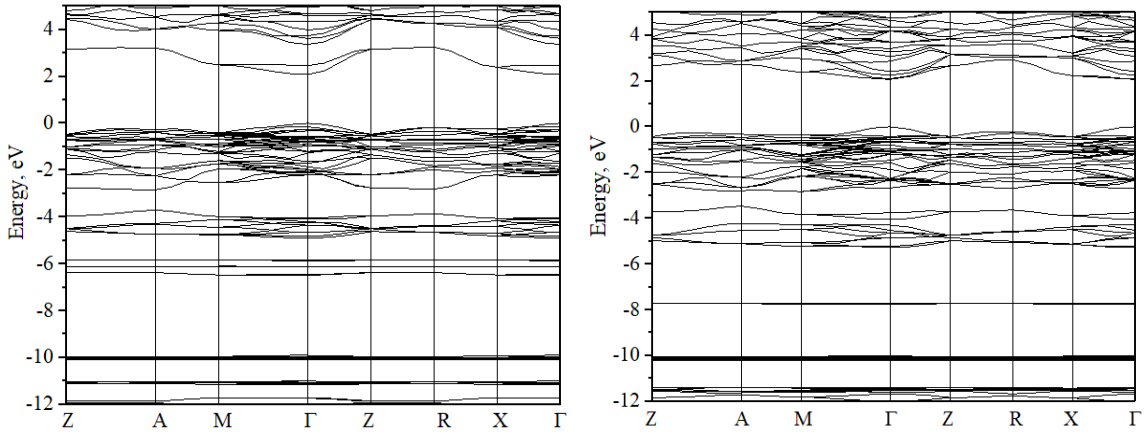

1 2

Fig. 2. Band energy diagram of the Tl_4HgI_6 (1) [13] and Tl_4CdI_6 (2) [6] crystals.

A value of $E_{cut\text{-}off}$= 310 eV for the energy of cutting-off the plane waves was used in calculations. The electron configurations of atoms are as follows: Tl — [Xe] $5d^{10}6s^26p^1$, I — [Kr] $5s^25p^5$, Hg — [Xe] $5d^{10}6s^2$, Cd — [Kr] $4d^{10}5s^2$ where [Kr] and [Xe] denote the inner core states. The integration over the Brillouin zone was performed on the 2×2×2 grid of *k* points by the Monkhorsta–Pack scheme [18]. A self-consistent convergence of the total energy was taken as 5.0×10^{-7} eV/atom. Geometric optimizations of the lattice parameters and the atomic coordinates were performed using a Broyden–Fletcher–Goldfarb–Shanno minimization technique. The maximal ionic Hellmann–Feynman forces were set within 0.01 eV/Å, the maximum ionic displacement within 5.0×10^{-4} Å, and the maximum stress within 0.02 GPa.

Table 1

Comparison of the experimental and equilibrium theoretical lattice parameters for A_4BX_6 group crystals

Crystal	*a*, nm	*b*, nm	*c*, nm
Tl_4HgI_6	0.9446 [7] 0.9664	0.9446 [7] 0.9664	0.92600 [7] 0.9524
Tl_4CdI_6	0.9231 [7] 0.9225	0.9231 [7] 0.9225	0.9592 [7] 0.9597

The simplest way to obtain data similar to the experimental ones is to use a so-called scissors operator, which changes the band gap by shifting the conduction bands toward higher energies [19]. This operator is based on the similarity of the dispersion dependences of the conduction band energies $E(\mathbf{k})$ determined by solving the Kohn–Sham equations [20]. The conduction bands of the calculated energy spectrum are usually shifted until they coincide with the experimental minimum energy gap E_g of the crystal.

II. Results and Discussion

Figure 2 shows the full energy band diagrams of the A_4BX_6 group crystals along the high-symmetry lines of the tetragonal Brillouin zone. Here, the energy is counted from the Fermi level.

The energy band diagram was constructed using the points of the Brillouin zone in the inverse space, which were as follows: Z(0, 0, 0.5), A(0.5, 0.5, 0.5), M(0.5, 0.5, 0), Γ(0, 0, 0), R(0, 0.5, 0.5), X(0, 0.5, 0).

An analysis of the results of theoretical calculations of the energy band spectrum shows that the smallest energy bandgap is localized in the center zone of the Brillouin zone (point Γ). This means that the crystal is

characterized by a direct energy bandgap.

The calculated value of the band gap E_g of Tl_4HgI_6 and Tl_4CdI_6 is estimated as 1.27 eV and 2.02 eV, respectively. In this relation, it is well known that DFT-based calculations of semiconductors in the LDA and GGA levels of theory usually underestimate the band gap E_g [19]. Using the experimental data of the band gap (E_g = 2.08 eV [5] for Tl_4HgI_6 and E_g = 2.83 eV [6] for Tl_4CdI_6) we have obtained the value of "scissor" factor being equal to 0.81 eV (the "scissor" factor may be used for comparison of theoretical and experimental optical spectra in the range of electron excitations).

When studying the optical properties, it is convenient to use complex dielectric function ε. Its imaginary part ε_2 can be calculated from the momentum matrix elements between the occupied and unoccupied wave functions [13]. Real part ε_1 of the dielectric function can be found from its imaginary part using the known Kramers–Kronig relationship [13]. Using the relationship:

$$n = \sqrt{\frac{(\varepsilon_1^2 + \varepsilon_2^2)^{1/2} + \varepsilon_1}{2}}, \qquad 1$$

as well as the calculated spectra of the real and imaginary parts of the dielectric function, the spectral dependences of the refractive index was found (Fig. 3). As can be seen from Fig. 3, the refractive indices satisfy the relation $n_c > n_{a,b}$ above 400 nm.

It can be seen that in the main spectral transmission region the refractive index increases towards shorter wavelength [21-29]. Such a behavior can be caused by increasing the exciton-phonon interaction and contribution of absorption coefficient in the process of formation of fundamental absorption edge.

Figure 4 presents the calculated anisotropic BRF dispersion for the A_4BX_6 crystals. The theoretical spectra show very good agreement with the experiment [13]. It is seen that the dispersion is normal ($d\Delta n/d\lambda < 0$) and the variation in the BRF itself with the wavelength is considerable ($d\Delta n/d\lambda \sim -3.03\times10^{-4}$ nm^{-1} for Tl_4HgI_6 and $d\Delta n/d\lambda \sim -1.1\times10^{-5}$ nm^{-1} for Tl_4CdI_6).

The anomalous by large values of difference ($\Delta n > 0.18$ for Tl_4HgI_6 and $\Delta n > 0.03$ for Tl_4CdI_6) of the BRF attract our attention for visible region of light. To our mind this behavior is caused by strong anisotropy of the optical functions ε_1, ε_2 [14]. For A_4BX_6 crystals, a comparison of BRF with other known crystals was given

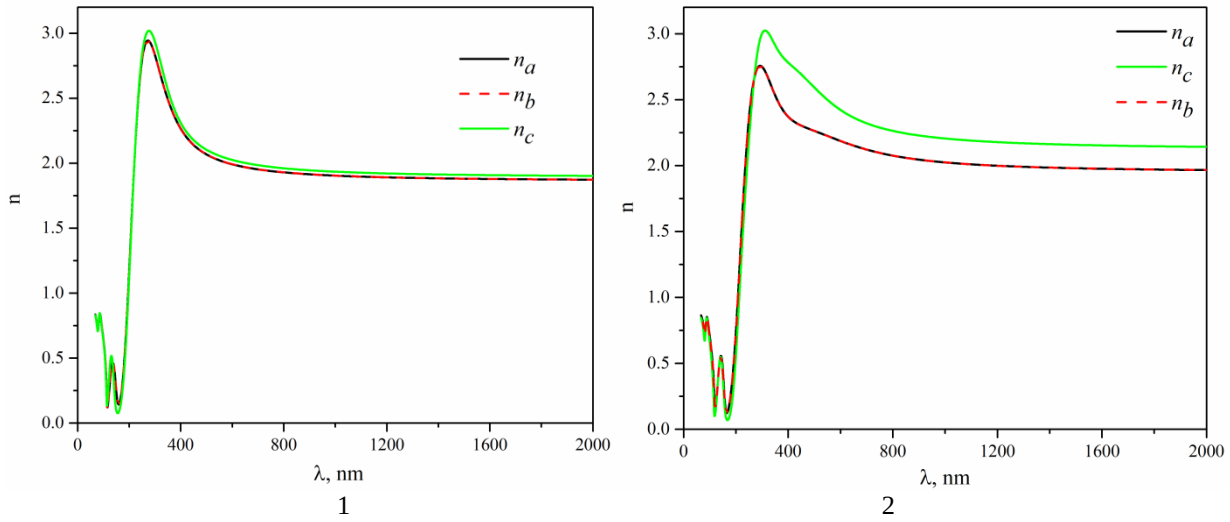

Fig. 3. Calculated spectra of the refractive index for three major crystallooptical directions of the Tl_4CdI_6 (1) and Tl_4HgI_6 (2) crystals.

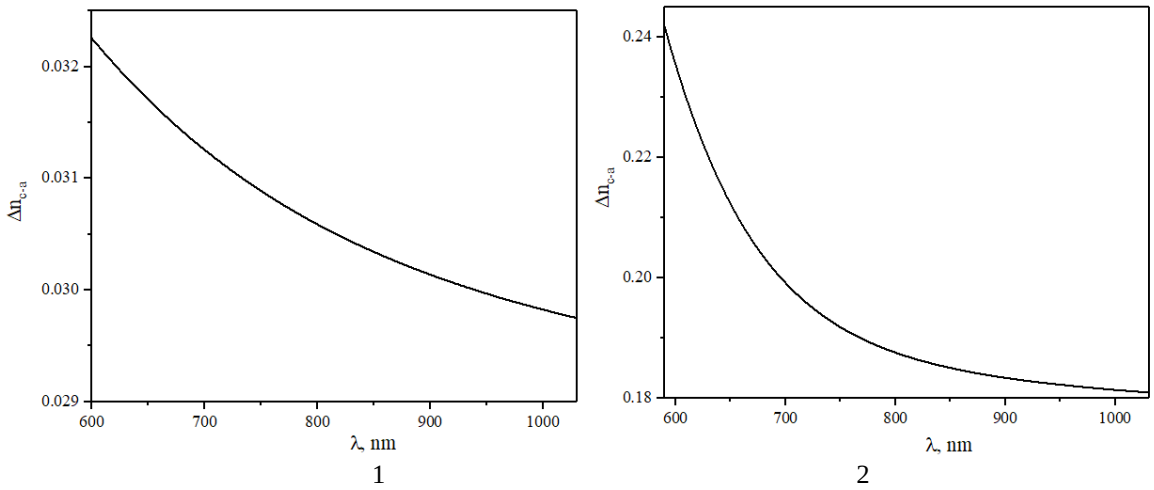

Fig. 4. Calculated spectra of BRF $\Delta n(\lambda)$ for Tl_4CdI_6 (1) and Tl_4HgI_6 (2) crystals.

Table 2

Comparison of the BRF for A_4BX_6 crystals with other known crystals

Crystal	Crystal structure	BRF (Δn)	Density, g/cm^3
$CaCO_3$*	Hexagonal	-0.172	2.715
TeO_2*	Hexagonal	-0.118	5.99
$LiNbO_3$*	Hexagonal	-0.086	4.65
SiO_2*	Hexagonal	+0.009	2.66
$In_{0.5}Tl_{0.5}I$	Orthorhombic	+0.255 [27]	6.234(2) [30]
$K_{1.75}(NH_4)_{0.25}SO_4$ [31]	Orthorhombic	+0.00237	2.539
$LiNaSO_4$ [32]	Hexagonal	+0.0046	2.525
Tl_4HgI_6	Hexagonal	+0.235	7.19 [7]
Tl_4HgI_6	Hexagonal	+0.269 [13]	7.19 [13]
Tl_4CdI_6	Hexagonal	+0.032	6.87 [6]

**data taken from Ref. [33]*

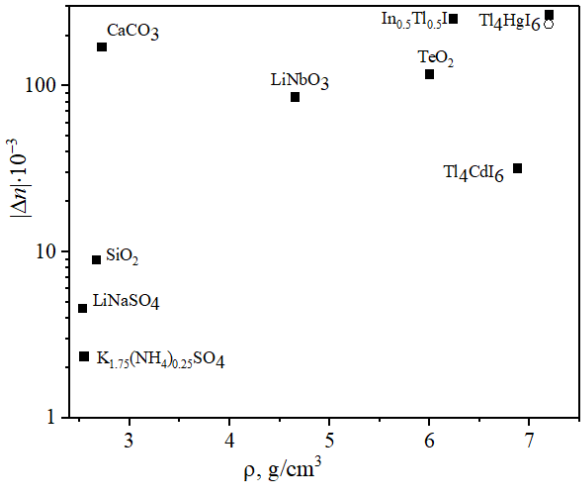

Fig. 5. Dependence of $|\Delta n| \sim f(\rho)$ for listed crystals from Table 2 (open circle at Tl_4HgI_6 correspond to our data).

in Table 2 (at room temperature for $\lambda \sim 600$ nm). Dependence of $|\Delta n| \sim f(\rho)$ for listed crystals from Table I present on Fig. 5.

Conclusion

The calculations of the energy band structure and optical spectra of a A_4BX_6 crystals within the framework of density functional theory allow us to make the following conclusions. It was established from the energy band diagrams that the minimum band gap is localized at the center of the Brillouin zone (at the Γ point). This means that the crystals are direct-gap. The spectral dependence of the refractive index was calculated on the basis of the energy band results with using the Kramers–Kronig method. It was found the anomalous by large values of the BRF in the visible and near infrared region (600 - 1100 nm).

Acknowledgments

In this work, for calculation was using QUANTUM-ESPRESSO package [34].

Ilchuk H. –Sc.D., Profesor at the Department of General Physics;
Solovyov M. – Junior Research Fellow at the Department of General Physics;
Lopatynskyi I. – Ph.D, Profesor at the Department of General Physics;
Honchar F. – Ph.D, Docent at the Department of General Physics;
Tsyupko F. – Ph.D., Docent at the Departments of Physical, Analytical and General Chemistry.

[1] D.S. Kalyagin, Y.E. Ermolenko and Y.G. Vlasov, Russ. J. Appl. Chem. 81(81), 2172 (2008) (DOI: 10.1134/S1070427208120264).
[2] D. Kahler, N.B. Singh, D.J. Knuteson, B. Wagner, A. Berghmans, S. McLaughlin, M. King, K. Schwartz, D. Suhre and M. Gotlieb, Nucl. Instruments Methods Phys. Res. Sect. A Accel. Spectrometers, Detect. Assoc. Equip. 652(1), 183 (2011) (DOI: 10.1016/j.nima.2010.09.057).
[3] K.I. Avdienko, D.V. Badikov, V.V. Badikov, V.I. Chizhikov, V.L. Panyutin, G.S. Shevyrdyaeva, S.I. Scherbakov and E.S. Scherbakova, Opt. Mater. (Amst). 23(3-4), 569 (2003) (DOI: 10.1016/S0925-3467(03)00023-5).
[4] S. Wang, Z. Liu, J.A. Peters, M. Sebastian, S.L. Nguyen, C.D. Malliakas, C.C. Stoumpos, J. Im, A.J. Freeman, B.W. Wessels and M.G. Kanatzidis, Cryst. Growth Des. 14(5), 2401 (2014) (DOI: 10.1021/cg5001446).
[5] V. Franiv, Visnyk of the Lviv University, Series Physics 48, 159 (2013).
[6] A.I. Kashuba, T.S. Malyi, M.V. Solovyov, V.B. Stakhura, M.O. Chylii, P. Shchepanskyi and V.A. Franiv, Optics and Spectroscopy 125(6), 853 (2018) (DOI: 10.1134/S0030400X18120081).

[7] A.I. Kashuba, M.V. Solovyov, T.S. Maliy, I.A. Franiv, O.O. Gomonnai, O.V. Bovgyra, O.V. Futey, A.V. Franiv and V.B. Stakhura, Journal of physical studies 22(2), 2701(1-4) (2014) (DOI: 10.30970/jps.22.2701).
[8] V.A. Franiv, Z. Czapla, S. Dacko, A.V. Franiv and O.S. Kushnir, Ukr. J. Phys. 59(11), 1078 (2014).
[9] M. Piasecki, G. Lakshminarayana, A.O. Fedorchuk, O.S. Kushnir, V.A. Franiv, A.V. Franiv, G. Myronchuk and K.J. Plucinski, J. Mater. Sci. Mater. Electron. 24(4), 1187 (2013) (DOI: 10.1134/S0030400X17070074).
[10] M. Solovyov, A. Kashuba, V. Franiv, A. Franiv and O. Futey, in Proceedings of the IEEE International Young Scientific Forum on Appl. Phys. Engineer, pp. 17-20, October 2017 (DOI: 10.1109/YSF.2017.8126617).
[11] A.I. Kashuba, M.V. Solovyov, A.V. Franiv, B. Andriyevsky, T.S. Malyi, V.B. Tsyumra, Ya.A. Zhydachevskyy, H.A. Ilchuk and M.V. Fedula, Low Temperature Physics 46(10), 1039 (2020) (DOI: 10.1063/10.0001922).
[12] A.I. Kashuba, R.Yu. Petrus, B.V. Andrievskyi, M.V. Solov'ev, I.V. Semkiv, T.S. Malyi, M.O. Chylii, V.B. Stakhura, P.A. Shchepanskyi and A.V. Franiv, Materials Science 55(4), 602 (2020) (DOI: 10.1007/s11003-020-00345-w).
[13] A. Kashuba, M. Solovyov, T. Malyi, I. Semkiv and A. Franiv, in Proceedings of XIth International Scientific and Practical Conference on Electronics and Information Technologies (ELIT), pp. 272–276, September 2019. (DOI: 10.1109/ELIT.2019.8892315).
[14] V. Franiv, O. Bovgyra, O. Kushnir, A. Franiv and K. J. Plucinski, Opt. Appl., XLIV(2), 317 (2014) (DOI: 10.5277/oa140212).
[15] D. Vanderbilt, Phys. Rev. B. 41(11), 7892 (1990) (DOI: 10.1103/PhysRevB.41.7892).
[16] J.P. Perdew, K. Burke, and M. Ernzerhof, Phys. Rev. Lett., 78(7), 1396 (1997) (DOI: 10.1103/PhysRevLett.78.1396).
[17] I.V. Semkiv, B.A. Lukiyanets, H.A. Ilchuk, R. Yu. Petrus, A.I. Kashuba and M.V. Chekaylo, J. Nano-Electron. Phys. 8(1), 01011(1-5) (2016) (DOI: 10.21272/jnep.8(1).01011).
[18] H.J. Monkhorst and J.D. Pack, Phys. Rev. B. 13(12), 5188 (1976) (DOI: 10.1103/PhysRevB.13.5188).
[19] A. Kashuba, B. Andriyevskyy, I. Semkiv, L. Andriyevska, R. Petrus, E. Zmiiovska and D. Popovych, J. Nano-Electron. Phys. 10(6), 06025(1-4) (2018) (DOI: 10.21272/jnep.10(6).06025).
[20] W. Kohn and L.J. Sham, Phys. Rev. A. 140(4), 1133 (1965) (DOI: 10.1103/PhysRev.140.A1133).
[21] R.Yu. Petrus, H.A. Ilchuk, A.I. Kashuba, I.V. Semkiv, E.O. Zmiiovska and F.M. Honchar, Journal of Applied Spectroscopy 87(1), 35 (2020) (DOI: 10.1007/s10812-020-00959-7).
[22] H. Ilchuk, R. Petrus, A. Kashuba, I. Semkiv and E. Zmiiovska, Molecular Crystals and Liquid Crystals 699(1), 1 (2020) (DOI: 10.1080/15421406.2020.1732532).
[23] R. Petrus, H. Ilchuk, A. Kashuba, I. Semkiv and E. Zmiiovska, Funct. Mater. 27(2), 342 (2020) (DOI: 10.15407/fm27.02.342).
[24] Z.R. Zapukhlyak, L.I. Nykyruy, V.M. Rubish, G. Wisz, V.V. Prokopiv, M.O. Halushchak, I.M. Lishchynsky, L.O. Katanova and R.S. Yavorskyi, Physics and Chemistry of Solid State 21(4), 660 (2020) (DOI: 10.15330/pcss.21.4.660-668).
[25] H.A. Ilchuk, A.I. Kashuba, R.Y. Petrus, I.V. Semkiv and V.G. Haiduchok, Journal of Physical Studies 24(3), 3705(9) (2020) (DOI: 10.30970/jps.24.3705).
[26] R. Yavorskyi, L. Nykyruy, G. Wisz, P. Potera, S. Adamiak, and S. Górny, Applied Nanoscience 9(5), 715 (2019) (DOI: 10.1007/s13204-018-0872-z).
[27] A.V. Franiv, V.Y. Stadnyk, A.I. Kashuba, R.S. Brezvin, O.V. Bovgira and A.V. Futei, Optics and Spectroscopy 123(1), 177(2017) (DOI: 10.1134/S0030400X17070074).
[28] A.I. Kashuba, A.V. Franiv, R.S. Brezvin and O.V. Bovgyra, Functional materials 23(4), 26 (2017) (DOI: 10.15407/fm24.01.026).
[29] L. Nykyrui, Y. Saliy, R. Yavorskyi, Ya. Yavorskyi, V. Schenderovsky, G. Wisz, and S. Górny, in 2017 IEEE 7th International Conference Nanomaterials: Application & Properties (NAP), pp. 01PCSI26-1, September 2017 (DOI: 10.1109/NAP.2017.8190161).
[30] A.I. Kashuba and S.V. Apunevych, J. Nano- Electron. Phys., 8(1), 1010(1-5) (2016) (DOI: 10.21272/jnep.10(1).01013).
[31] P.A. Shchepanskyi, O.S. Kushnir, V.Yo. Stadnyk, A.O. Fedorchuk, M.Ya. Rudysh, R.S. Brezvin, P.Yu. Demchenko and A.S. Krymus, Ukr. J. Phys. Opt., 18(4), 187 (2017) (DOI: 10.3116/16091833/18/4/187/2017).
[32] P.A. Shchepanskyi, O.S. Kushnir, V.Yo. Stadnyk, R.S. Brezvin and A.O. Fedorchuk, Ukr. J. Phys. Opt. 19(3), 141 (2018) (DOI: 10.3116/16091833/19/3/141/2018).
[33] http://www.mt-berlin.com/frames_cryst/descriptions/birefringent.htm.
[34] P. Giannozzi, O. Andreussi, T. Brumme, O. Bunau, M.B. Nardelli, M. Calandra, R. Car, C. Cavazzoni, D. Ceresoli, and M. Cococcioni, J. Phys. Condens. Matter. 29, 465901 (2017) (DOI: 10.1088/1361-648X/aa8f79).

H. Ilchuk, M. Solovyov, I. Lopatynskyi, F. Honchar, F. Tsyupko

Г. Ільчук, М. Соловйов, І. Лопатинський, Ф. Гончар, Ф. Цюпко

Оптичні властивості кристалів групи A_4BX_6: розрахунок з перших принципів

Національний університет "Львівська політехніка", Львів, Україна, mvsolovyov@ukr.net

Представлено результати дослідження електронної енергетичної структури та оптичних властивостей кристалів групи A_4BX_6 (Tl_4HgI_6 та Tl_4CdI_6). Електронна енергетична структура кристалів Tl_4HgI_6 та Tl_4CdI_6 обчислюється за першими принципами в рамках узагальненого градієнта апроксимації (GGA). Зонну структуру та показник заломлення розраховували за допомогою псевдопотенційного методу в рамках теорії функціоналу густини. Край оптичного поглинання в Tl_4HgI_6 та Tl_4CdI_6 сформований прямими оптичними переходами. Спектральну залежність показника заломлення розраховували на основі результатів електронної енергетичної структури за допомогою методу Крамерса – Кроніга. Спектри демонструють виражену анізотропію в поляризаціях $E\|\boldsymbol{a}(\boldsymbol{b})$ та $E\|\boldsymbol{c}$. Виявлено аномально велике значення показника двопроменезаломлення ($\Delta n > 0.18$ for Tl_4HgI_6 and $\Delta n > 0.03$ for Tl_4CdI_6) у видимій та ближній інфрачервоній області.

Ключові слова: оптичні константи, двопроменезаломлення, електронна енергетична структура.